Using Grote−Hynes Theory To Quantify Dynamical Effects on the Reaction Rate of Enzymatic Processes. The Case of Methyltransferases†

Raquel Castillo,‡ Maite Roca,§ Alejandro Soriano,|| Vicente Moliner,*,‡ and Iñaki Tuñón*,||

Departamento de Química Física y Analítica, Universidad Jaume I, 12071 Castellón, Spain, Department of Chemistry, University of Southern California, Los Angeles, California 90089-1062, and Departamento de Química Física, Universidad de Valencia, 46100 Burjassot, Spain

Received: September 24, 2007; In Final Form: November 14, 2007

Dynamical effects have recently received much attention in the context of the theoretical investigation of enzymatic catalysis. In this paper we use a combination of Grote−Hynes theory with quantum mechanical/molecular mechanical modeling that is a powerful tool to understand and quantify these dynamical effects in a particular enzyme, the glycine *N*-methyltransferase (GNMT). Comparison of the results obtained for this enzyme with another methyltransferase (catechol *O*-methyltransferase, COMT) allows us to understand the different nature of the coupling of the environment to the reaction coordinate as a function of the electrostatic interaction established by the reactive subsystem. The transmission coefficients obtained using Grote−Hynes theory are in excellent agreement with molecular dynamics estimations and show that the coupling is higher in GNMT than in COMT. The larger friction observed in GNMT is explained on the basis of the interaction established by the substrate in the active site. The larger value of the friction leads to a smaller value of the reaction frequency and thus also to a larger disagreement with the estimation of the transmission coefficient based on the frozen environment approach.

1. Introduction

Computational simulations of enzymatic processes have become a decisive tool to investigate into the origins of the amazing catalytic power of these proteins.[1−5] From these studies many proposals have been put forward to rationalize the rate acceleration observed relative to the counterpart process in aqueous solution. One of these proposals has been the existence of specific dynamical effects favoring the reaction in the active site. The essence of the idea is the existence of particular vibrational motions in the enzyme that could promote the transformation from the reactant to the transition state.[6] In other words, the internal motions of the protein should be significantly coupled to the reaction coordinate that defines the internal changes in the chemical system.[7] The study of the protein-reaction coupling has received considerable attention,[6−10] using terms such as "protein promoting vibrations",[8] and may be very useful to reveal the details of the reaction dynamics in complex media.[11] However, it must be noticed that to have a contribution to catalysis, these dynamical effects should make a quite different contribution to the reaction rate in aqueous solution and in the enzyme.[12]

To verify these hypotheses, it is important to use theoretical approaches able to quantify these "dynamical effects" for the reaction in aqueous solution and in the enzyme. There are several approaches that quantify the dynamical effects, for instance the dispersed polaron (DP) (spin Boson) method.[13] Grote−Hynes (GH) theory[14−16] provides an adequate framework to estimate the contribution of dynamical effects to catalysis and to gain better understanding of the coupling between the protein and reaction dynamics in enzymatic processes. This theory is derived under the assumptions of quadratic potential, bilinear coupling, and classical behavior of the motion along the reaction coordinate. The application of this theory requires of the evaluation of the friction kernel in the transition state. This friction kernel is obtained from the averaged forces exerted on a distinguished reaction coordinate by the remaining degrees of freedom of the system and thus it gives a quantitative estimation of the coupling between the reaction coordinate and the environment.[13] Using the generalized Langevin equation,[14−16] it is possible to estimate the transmission coefficient of the reaction and thus compare the contribution of "dynamical effects" to the reaction rate in solution and in the enzyme. Moreover, we have shown that combining the Fourier transform of the friction kernel with normal mode calculations,[17] one can identify the more relevant vibrational motions, in terms of coupling with the reaction coordinate. Finally, it is also possible to classify the vibrational motions of the environment as active or inactive, depending on the value of their characteristic frequencies as compared to the reaction frequency. Inactive motions remain essentially frozen during the barrier passage, whereas active motions are able to follow the evolution of the system along the reaction coordinate.[15]

We have previously shown that GH theory can be successfully applied to the analysis of enzymatic reactions combined with quantum mechanical/molecular mechanical (QM/MM) simulations. In particular, we previously applied GH theory to the reactions catalyzed by catechol *O*-methyltransferase (COMT)[17] and chalcone isomerase (CHI).[18] In both cases GH theory provides values of the transmission coefficient in excellent agreement with MD estimations, for the reactions both in the enzyme and in aqueous solution. In this paper, GH theory is applied to another methyltransferase (glycine *N*-methyltrans-

† Part of the "James T. (Casey) Hynes Festschrift".

* Corresponding authors. E-mail: V.M., moliner@qfa.uji.es; I.T., tunon@uv.es.

‡ Universidad Jaume I.

§ University of Southern California.

|| Universidad de Valencia.

10.1021/jp077660b CCC: $40.75
Published on Web 12/18/2007

SCHEME 1

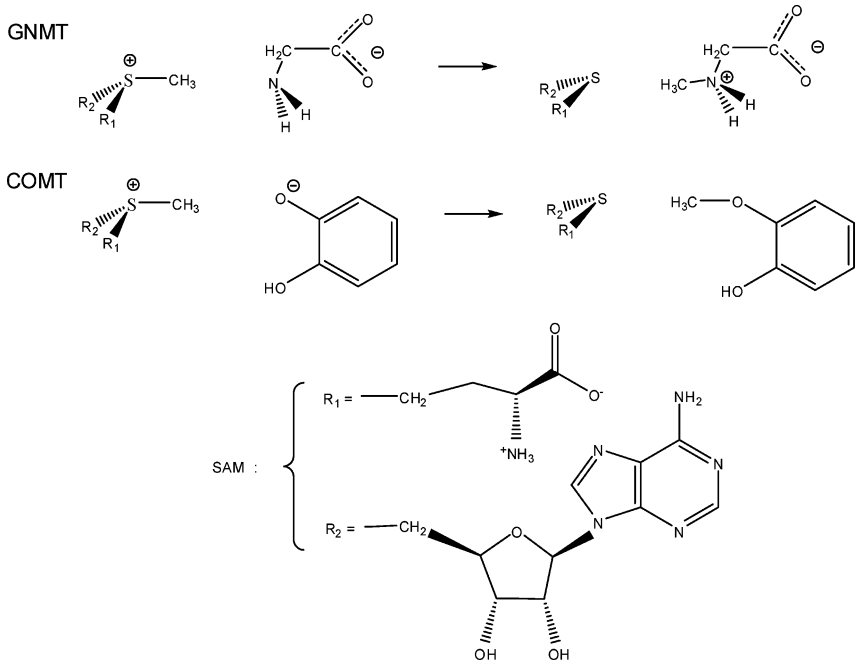

ferase or GNMT). This enzyme catalyzes a methyl transfer from *S*-adenosylmethionine (SAM), which is a cofactor used by many methyltransferases (such as COMT),[19] to the substrate, glycine, thus converting it into sarcosine.[20] The purpose of this study is to be able to rationalize the behavior of the environment in two reactions that are formally very similar but differing in the charge variation associated with the reaction progress. Thus, whereas COMT catalyzed reaction takes place from charged reactants to neutral products, the reaction catalyzed by GNMT takes place from charged reactants to polar products. This is, in the first case a dipole moment is annihilated, whereas in the second one the dipole moment of the reactant system is not completely vanished as the reaction proceeds (see Scheme 1). In both cases electrostatic effects of the environment seem to be the key factor to understand catalysis.[21,22] These results can be viewed in a more general perspective of enzymatic catalysis based on the electrostatic stabilization of the transition state as compared to the aqueous solution reaction.[23] Nevertheless, the different nature of the reactions in terms of electrostatic interactions with the environment suggests that a comparative analysis of "dynamical effects" based on the use of GH theory can be very illustrative.

2. Methodology

2.1. Hybrid QM/MM Model. Details of the computational model are given in our previous paper about GNMT.[22] Briefly, to study the reaction catalyzed by GNMT and its counterpart process in aqueous solution, we have used the QM/MM methodology[24−27] by means of the DYNAMO program.[28] The SAM molecule and the glycine were chosen to be the QM subsystem, and the rest of the enzyme and/or water molecules are in the MM subsystem. We used the semiempirical Hamiltonian AM1[29] to describe the QM subsystem. The MM subsystem was treated using the OPLS-AA force field[30] for the enzyme atoms, amd the TIP3P potential[31] was used for the water molecules. A switched cutoff radius of 12 Å was used for all kind of interactions.

For studying the enzyme reaction, the initial atomic coordinates were taken from the X-ray crystal structure with Protein Data Bank code 1NBH.[32] The enzymatic system (enzyme plus SAM plus substrate) was placed in a cavity deleted from a 79.5 Å side box of TIP3P water molecules. All atoms beyond 25 Å of any atom of the SAM or glycine molecule were kept frozen (41 399 atoms in total). To study the reaction in aqueous solution, SAM and glycine were placed in the center of a 79.5 Å side box of water molecules, deleting those overlapping with the reactant molecules. The final number of water molecules was 16801. Periodic boundary conditions and a temperature of 300 K were used during all the simulations.

Both in aqueous solution and in the enzyme the glycine was described as a zwitterion. In our previous work we proved this to be the preferred ionization state in this reaction.[22] The free energy profiles were obtained in terms of a distinguished reaction coordinate defined as the difference between the bond breaking (C−S) and bond forming (C−N) distances. The same coordinate was used in the case of COMT.[21]

2.2. Application of Grote−Hynes Theory. In GH theory the transmission coefficient can be obtained as the ratio between the reactive frequency and the frequency obtained under the assumption of equilibrium between the reaction coordinate and the rest of degrees of freedom:[15]

$$\kappa_{GH} = \frac{\omega_r}{\omega_{eq}} \tag{1}$$

The equilibrium frequency can be obtained from the curvature of the reaction free energy profile obtained under the equilibrium assumption along a particular reaction coordinate (in this case the antisymmetric combination of bond breaking and bond forming distances). The reactive frequency can be obtained making use of the GH equation:[14,15]

$$\omega_r^2 - \omega_{eq}^2 + \omega_r \int_0^\infty \zeta_{TS}(t) e^{-\omega_r t}\, dt = 0 \tag{2}$$

where $\zeta_{TS}(t)$ is the friction kernel evaluated in the transition state (TS).[16] The analysis of the friction kernel, which gives the fluctuating forces acting on the reaction coordinate, provides an efficient way to quantify the coupling of the rest of degrees of freedom of the system with the selected reaction coordinate.

This friction can be evaluated from the autocorrelation function of the forces acting on the reaction coordinate:[15,33]

$$\zeta(t) = \frac{\langle F_{RC}(0)\, F_{RC}(t)\rangle}{\mu_{RC} k_B T} \quad (3)$$

where $F_{RC}(t)$ is the force on the reaction coordinate and μ_{RC} is the associated reduced mass. With this purpose we ran 100 ps of constrained MD simulations at the top of the Potential of Mean Force (PMF), using a Wilson's matrix based RATTLE-like velocity-Verlet algorithm at 300 K.[34,35] A very small time step of 0.1 fs was used to ensure the convergence of the algorithm. Forces acting on the reaction coordinate were saved at each simulation step.

2.3. Rare Event Trajectories. NVT MD trajectories (500 ps long) restrained in the TS region with a time step of 0.5 fs have been carried out following a protocol used in other enzymatic reactions.[36,37] The simulation temperature was 300 K and configurations were saved at 5 ps intervals, resulting in 100 configurations that were used to compute free downhill trajectories. Because the velocity associated with the reaction coordinate is not properly thermalized in these configurations, several strategies are possible to obtain suitable velocities for the starting points.[38] We selected an approximation of velocity randomization based on the fact that the system may be represented by different fragments, A−B−C−D (A = methyl group, B = cofactor SAM except methyl group, C = glycine, D = the rest of the system). The translation velocities of the centers of mass of the fragments were assigned to a random value from Maxwell−Boltzmann distribution at 300 K, preserving thus the velocities of the other degrees of freedom.[39] This procedure has been successfully employed in previous studies of enzymatic and aqueous solution reactions providing a set of well-behaved reactive trajectories.[36−38] Once the randomized velocities were obtained for each selected TS configuration, the downhill trajectories were computed, releasing the restraint previously imposed on the reaction coordinate that kept the structure in the region of the TS. The equations of motion were integrated forward and backward in time, multiplying the velocities by one, for forward integration, and by minus one, for backward integration.[40] Downhill trajectories were propagated from −2 to +2 ps using a time step of 0.5 fs. The trajectories obtained in the enzyme and in solution were then classified as reactive trajectories, when reactants connect to products (RP trajectories) and nonreactive otherwise. In this last case we found trajectories leading from reactants to reactants (RR) or from products to products (PP). To compute the transmission coefficient, we used the "positive flux" formulation,[39] assuming that the trajectory is initiated at the barrier top with forward momentum along the reaction coordinate:

$$\kappa(t) = \frac{\langle j_+ \theta[\mathrm{RC}(+t)]\rangle - \langle j_+ \theta[\mathrm{RC}(-t)]\rangle}{\langle j_+\rangle} \quad (4)$$

where j_+ is the initial positive flux at $t = 0$ and θ(RC) is a step function equal to 1 in the product side of the reaction coordinate and 0 on the reactant side. The averaged time-dependent transmission coefficient is calculated over all the downhill trajectories.

3. Results

Rare event trajectories are classified in such a way that they have positive velocities in the reaction coordinate at $t = 0$, which sends them toward products at positive times ($t > 0$), and negative velocities, which sends them toward reactants at negative times ($t < 0$). A significant fraction of the 100 trajectories presented recrossings of the transition state dividing surface. Thus, they have been classified as (i) direct reactant-product (RP) trajectories, (ii) trajectories leading from reactants to reactants (RR), and (iii) trajectories leading from products to products (PP). For GNMT we observed 49 trajectories of RP type, 26 of RR type, and 33 of PP type.

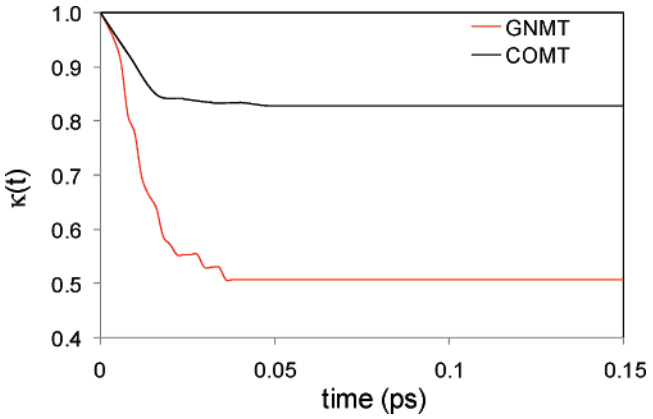

Figure 1. Time-dependent transmission coefficients obtained from rare-event reaction trajectories in GNMT and COMT.

TABLE 1: Transmission Coefficients Obtained from Molecular Dynamics (κ_{MD}), Grote−Hynes Theory (κ_{GH}), Frozen Environment Approach (κ_{fe}), and Kramers Regime (κ_{Kr}) in GNMT and COMT

	κ_{MD}	κ_{GH}	κ_{fe}	κ_{Kr}
GNMT	0.51 ± 0.05	0.55 ± 0.04	0.31	0.01
COMT	0.83 ± 0.03	0.89 ± 0.03	0.86	0.10

Because of the existence of recrossings in the trajectories crossing over the transition state defined in terms of the distinguished reaction coordinate, the rate constant deduced from the transition state theory needs to be corrected by a transmission coefficient, κ, which will necessarily be less than unity. The time-dependent transmission coefficient obtained for GNMT is represented in Figure 1, together with that obtained in the case of COMT.[17] The shape of the $\kappa(t)$ curves show a fast decay in both enzymes. It can be readily seen that the fate of the reaction is completely defined after the first 40 fs in GNMT and after 50 fs in COMT, in good agreement with other S_N2 reactions.[15] After this period of time, recrossings are not observed and the system evolves monotonically toward the corresponding valley. As observed in Figure 1, the transmission coefficient reaches a plateau, from which the value of the transmission coefficient can be obtained. The computed value of κ for the GNMT catalyzed reaction is 0.51 ± 0.05 (errors, expressed as a standard deviation, calculated according to ref 13). In the case of COMT we obtained a larger value for the transmission coefficient (0.83 ± 0.03), indicating a lower probability for a recrossing to occur in this enzyme.

Table 1 provides the values of the transmission coefficient obtained using GH theory. We have also calculated the transmission coefficients in two limits that can be derived from this theory.[15] The first one is the frozen environment (fe)[41−43] approach (or nonadiabatic limit) in which the remaining degrees of freedom of the system are assumed to be completely frozen during the passage of the system over the transition state. The second one is the Kramers regime[44] where all the friction is exerted during the barrier crossing. First, it is important to emphasize that, as in preceding examples commented in the introduction,[17,18] GH theory provides transmission coefficients

TABLE 2: Characteristic Frequencies (in cm^{-1}) for the Methylation Reaction in GNMT and COMT

	ω_{eq}	ω_r	w_z
GNMT	1170	640	1100
COMT	1200	1070	600

in excellent agreement with MD estimations, typically within one standard deviation. Thus, GH theory provides a computationally efficient tool to obtain this value in a much simpler way than running rare event reaction trajectories. These values of the transmission coefficient can be then safely used as a measure of the dynamic effects. Conversely, Kramers regime results in transmission coefficients clearly below the MD estimation. Using this regime, one could erroneously conclude that the "dynamic effects" make a significant contribution to the free energy barrier because the reaction rate constant is diminished, in this approach, in one or 2 orders of magnitude for the case of COMT and GNMT, respectively. The frozen environment approach results in a much more reasonable approximation, although assuming that all the degrees of freedom are kept frozen except the reaction coordinate can also lead to significant deviations if fast motions, strongly coupled to the reaction progress, are present in the system.

From the results obtained for the transmission coefficient, free energy contribution to the barrier is 0.4 and 0.1 kcal/mol, for GNMT and COMT, respectively. These results reflect that the influence of the "dynamical effects" on the rate constant is quite modest. Furthermore, as far as we know, there is no evidence of any system studied up to this moment of large differences between the transmission coefficients obtained for the catalyzed reaction and its counterpart process in aqueous solution.[18,36,37,45] For example, in the case of the reaction catalyzed by COMT the transmission coefficient in aqueous solution was found to be 0.62 ± 0.04.[17] Thus, one can conclude that the magnitude of the "dynamical effects" on catalysis is nearly negligible in COMT: the dynamical contribution to the increase in the rate constant when passing from aqueous solution to the enzyme (evaluated from the computed transmission coefficients) is 1.3 and the total rate constant is increased by several orders of magnitude (about 10^7).[21,46]

Once the performance of GH theory in the calculation of enzymatic transmission coefficients was established, we decided to use this theory to rationalize the differences observed between GNMT and COMT. Table 2 provides the characteristic frequencies of the methylation reaction in both COMT and GNMT. The equilibrium frequency (ω_{eq}) is derived from the curvature of the free energy profile in the region around the barrier top (as obtained in refs 15 and 16). The reaction frequency (ω_r) is the actual frequency of the system motion along the reaction coordinate. The ratio between these two magnitudes is the transmission coefficient. The friction frequency (ω_ζ) reflects the value of the initial friction expressed as a wavenumber:

$$\omega_\zeta = \frac{1}{2\pi c}\sqrt{\zeta(t=0)} \tag{5}$$

It is interesting to note that both processes have a very similar equilibrium frequency.

Nevertheless, by comparison of the reaction and friction frequency we can conclude that the differences observed in the values of the transmission coefficients of the reactions catalyzed by GNMT and COMT are due to the fact that the friction, or the coupling between the reaction coordinate and the remaining degrees of freedom of the system, is significantly larger in the former one. The normalized autocorrelation functions (ACFs) of the forces acting on the reaction coordinate in both enzymes are represented in Figure 2. This autocorrelation function determines the friction kernel, according to eq 3. In both cases the ACF shows a very rapid relaxation followed by fast oscillations. However, there are also noticeable differences between both ACFs. First, the relaxation is slower in GNMT than in COMT, as reflected by the value of the 1/e correlation time, which amounts to 170 fs in COMT and to 750 fs in GNMT. This correlation time, which is also a measure of the time scale of the environment movements, is in any case significantly larger than the time scale associated with the motion along the reaction coordinate, 5 and 8 fs in COMT and GNMT, respectively. Second, the fine structure of the ACFs is also different, reflecting the fact that the motions of the rest of degrees of freedom may contribute differently to the friction in each enzyme.

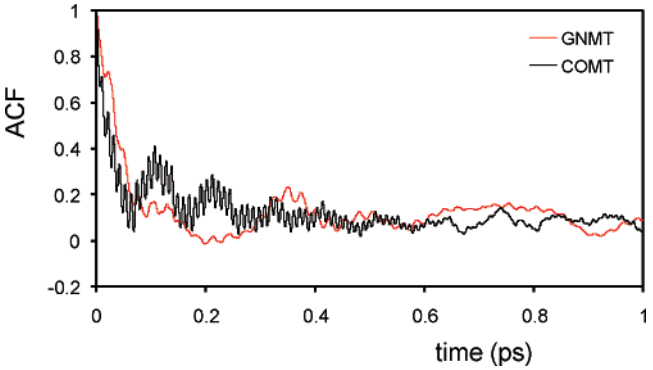

Figure 2. Normalized autocorrelation function of the force acting on the reaction coordinate in COMT and GNMT.

We can obtain the spectral distribution of the system and identify which motions couple to the reaction coordinate by means of the Fourier transform of the friction kernel:[15]

$$\zeta(\omega) = \int_{-\infty}^{+\infty} \zeta(t) e^{i\omega t}\, dt \tag{6}$$

The intensity of the signal informs about the degree of coupling to the reaction coordinate. The friction spectra are very useful for classifying the different motions coupled to the reaction coordinate depending on the value of their characteristic frequency.[3,14,47,48] Effectively, those motions with a frequencies significantly lower than the reaction frequency are expected to remain essentially frozen during the passage of the system over the barrier top. These motions contribute to the reaction recrossings because of their inactivity during the time scale of the reaction. Those motions appearing in the high-frequency region of the friction spectra (relative to the reaction frequency) are expected to become unfrozen and then dynamically influencing the recrossings, allowing the transmission coefficient to be larger than in the frozen environment approach. The friction spectra obtained in GNMT and COMT are presented in Figure 3. We can observe important differences between both spectra that we have rationalized in terms of the different role played by the charge of the substrate (glycine or catecholate) in each enzyme (GNMT or COMT, respectively). As can be seen in Scheme 1, both substrates have a negative charge. However, in the case of catecholate the negative charge is formally located on the oxygen atom acting as the methyl acceptor, whereas in the GNMT case the charge is formally found on the carboxylate group of glycine and remains essentially unaltered during the reaction. Thus, the effect of the substrate's charge on the reaction is essentially included in the reaction coordinate in the case of the COMT catalyzed reaction, whereas in the GNMT, this

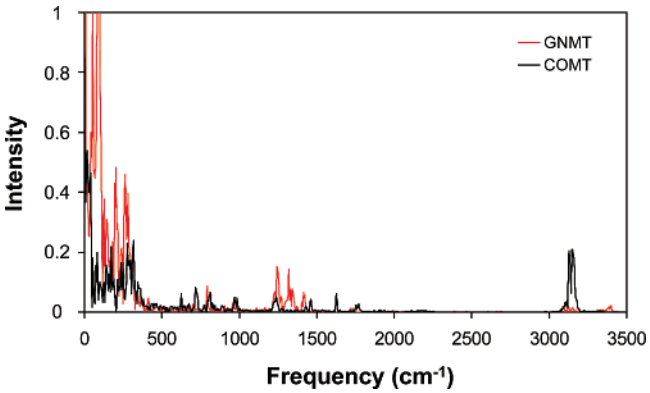

Figure 3. Friction spectra obtained in COMT and GNMT.

TABLE 3: AM1/MM Averaged Distances (in Å) and Angles (in Degrees) of the GNMT and COMT Transition State and Free Energy Barriers (kcal/mol)

	$\langle d_{S-C} \rangle$	$\langle d_{C-N} \rangle / \langle d_{C-O} \rangle$	S−C−N/S−C−O	$\Delta G^{\ddagger}$
GNMT	2.24	2.07	163.6	28.8
COMT	2.13	2.06	165.1	10.4

negative charge couples to the reaction progress through other coordinates (and thus the friction is higher and the transmission coefficient lower). The charge on the oxygen atom plays a fundamental role defining the interaction with the transferred methyl group in the transition state of COMT. Instead, for the transition state of GNMT, the interaction between the nitrogen atom and the methyl group is essentially due to the orbital overlapping between the lone pair of the nitrogen atom and the vacant orbital of the methyl group. This difference is clearly reflected in the geometrical characteristics of the transition states and the magnitude of the free energy barrier, gathered in Table 3. The transition state is more associative and the barrier height lower in the case of COMT. Thus, the transition state of GNMT is much more sensitive to relative motions of the glycine substrate that can lead to a significant loss of the correct orbital overlapping. These motions of the substrate inside the active site are clearly influenced by the charge−charge interaction established between the carboxylate group and Arg-175, which is hydrogen bonded to this moiety (a snapshot of the transition state in GNMT is shown in Figure 4). This kind of collective motions of the glycine molecule and the residues surrounding appears in the low-frequency region of the friction spectra (up to 500 cm^{-1}) and is responsible of the larger intensity observed in this region with respect to the case of COMT.

The low-frequency region of the friction spectra explains the fact that the transmission coefficient obtained under the frozen environment approach is significantly smaller for GNMT than for COMT. However, it must be also pointed out that this approach works significantly better for COMT. The reason is found in the fact that the reaction frequency is larger in this enzyme (1070 versus 640 cm^{-1}). Thus, there are more protein motions that can follow the changes in the reaction coordinate in GNMT than in COMT. The high-frequency regions of the friction spectra also display important differences in both cases. For example, the band appearing at 3100 cm^{-1}, associated with the C−H stretching of the transferred methyl group, is much more intense in the COMT spectrum. We attribute the different coupling of this motion to the reaction coordinate to the different associative/dissociative nature of the transition state in both enzymes. In the case of GNMT we also observe a small signal at about 3400 cm^{-1} that can be assigned to the stretching of the hydrogen atoms bonded to the nitrogen atom acting as methyl acceptor. This signal is obviously absent in the case of

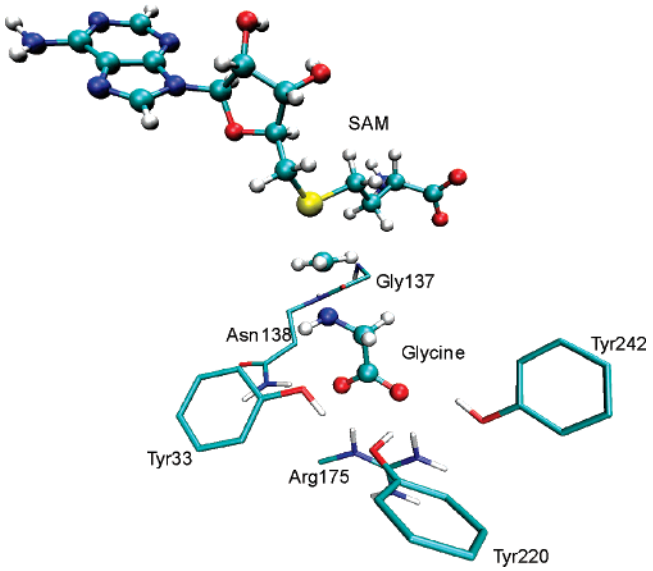

Figure 4. Snapshot of the transition state in GNMT.

COMT. Another signal that appears only in the GNMT spectrum (at about 1300 cm^{-1}) has been assigned to the bending motion of the NH_2 group of glycine, whereas the common signal found at about 1200 cm^{-1} is associated with the umbrella motion of the methyl group.

4. Conclusions

Using GH theory, we have been able to quantify the magnitude of "dynamical effects" on the GNMT reaction rate through the calculation of the friction kernel. This friction can be further decomposed to analyze the influence of different motions on the advance of the system along the reaction coordinate.

We have shown that GH theory can be used in combination with QM/MM methodology to gain a better understanding of the coupling between protein and substrate in enzymatic processes. In this paper, we have presented the application of this combined strategy to a methyl-transfer reaction catalyzed by GNMT. The value of the transmission coefficient obtained from GH theory is in excellent agreement with the value derived from rare-event reaction trajectories. Neither the Kramers regime nor the frozen environment approach are able to provide such good agreement.

We have also compared the results obtained for GNMT with another methyltransferase enzyme: COMT. The main difference between both systems is found in the fact that the negative charge of the substrate in the latter (catecholate) is formally found on the acceptor atom and then the reaction leads to dipole annihilation, whereas in GNMT the charge is found not on the methylated nitrogen atom of the glycine substrate but on the carboxylate group. Then the product is a zwitterion. As a consequence, the coupling of the remaining degrees of freedom of the system to the reaction coordinate is substantially larger in GNMT than in COMT and the reaction frequency is clearly diminished, resulting in a lower transmission coefficient.

The low-frequency region of the friction spectrum in GNMT shows many strong signals associated with the reorientational motions of the substrate and the hydrogen bond interactions established with the surrounding residues. The influence of the low-frequency region is reflected in the fact that the frozen environment transmission coefficient is lower in GNMT than in COMT. Simultaneously, because the reaction frequency in GNMT is lower than in COMT, the influence of active motions

(vibrations coupled to the reaction coordinate that can follow the evolution of the system through the barrier top) is larger and then the frozen environment approach works better in COMT than in GNMT.

Finally, it is possible to conclude that the different dynamical contribution to catalysts of the two studied methyltransferases, albeit representing a quite modest influence in the different rate constants, is in fact a consequence of the different electronic character of the chemical reaction they catalyze.

Acknowledgment. We are indebted to *Ministerio Educación y Ciencia* for projects CTQ2006-15447-C02-01 and CTQ2006-15447-CO2-02, *Generalitat Valenciana* for projects GV06-016, GV06/021 and 865/2006 and UJI-Bancaixa for project P1·1B2005-15 which supported this research. M.R. thanks Universitat Jaume I and the Generalitat Valenciana for the postdoctoral fellowships.

References and Notes

(1) Warshel, A. *Computer Modeling of Chemical Reactions in Enzymes and Solutions*; Wiley-Interscience: New York, 1991.
(2) Garcia-Viloca, M.; Gao, J.; Karplus, M.; Truhlar, D. G. *Science* **2004**, *303*, 186.
(3) Villa, J.; Warshel, A. *J. Phys. Chem. B* **2001**, *105*, 7887.
(4) Kollman, P. A.; Kuhn, B.; Donini, O.; Perakyla, M.; Stanton, R.; Bakowies, D. *Acc. Chem. Res.* **2001**, *34*, 72.
(5) Marti, S.; Roca, M.; Andres, J.; Moliner, V.; Silla, E.; Tuñón, I.; Bertran, J. *Chem. Soc. Rev.* **2004**, *33*, 98.
(6) Karplus, M.; Mccammon, J. A. *Annu. Rev. Biochem.* **1983**, *52*, 263.
(7) Neria, E.; Karplus, M. *Chem. Phys. Lett.* **1997**, *267*, 23.
(8) Antoniou, D.; Schwartz, S. D. *J. Phys. Chem. B* **2001**, *105*, 5553.
(9) Cui, Q. A.; Karplus, M. *J. Phys. Chem. B* **2002**, *106*, 7927.
(10) Basran, J.; Sutcliffe, M. J.; Scrutton, N. S. *Biochemistry* **1999**, *38*, 3218.
(11) Hammes-Schiffer, S. *Biochemistry* **2002**, *41*, 13335.
(12) Olsson, M. H. M.; Parson, W. W.; Warshel, A. *Chem. Rev.* **2006**, *106*, 1737.
(13) Warshel, A.; Chu, Z. T.; Parson, W. W. *Science* **1989**, *246*, 112.
(14) Grote, R. F.; Hynes, J. T. *J. Chem. Phys.* **1980**, *73*, 2715.
(15) Gertner, B. J.; Wilson, K. R.; Hynes, J. T. *J. Chem. Phys.* **1989**, *90*, 3537.
(16) Hynes, J. T. *The Theory of Chemical Reaction Dynamics*; Baer, M., Eds.; CRC: Boca Raton: FL, 1985; Vol. IV, p 171.
(17) Roca, M.; Moliner, V.; Tuñón, I.; Hynes, J. T. *J. Am. Chem. Soc.* **2006**, *128*, 6186.
(18) Ruiz-Pernia, J. J.; Tuñón, I.; Moliner, V.; Hynes, J. T.; Roca, M. Manuscript in preparation.
(19) Usdin, R.; Borchardt, R. T.; Creveling, C. R. *Transmethylation*; Elsevier-North-Holland: New York, 1979; Vol. 5.
(20) Blumenstein, J.; Williams, G. R. *Biochem. Biophys. Res. Commun.* **1960**, *3*, 259.
(21) Roca, M.; Marti, S.; Andres, J.; Moliner, V.; Tuñón, M.; Bertran, J.; Williams, A. H. *J. Am. Chem. Soc.* **2003**, *125*, 7726.
(22) Soriano, A.; Castillo, R.; Christov, C.; Andres, J.; Moliner, V.; Tuñón, I. *Biochemistry* **2006**, *45*, 14917.
(23) Warshel, A.; Sharma, P. K.; Kato, M.; Xiang, Y.; Liu, H. B.; Olsson, M. H. M. *Chem. Rev.* **2006**, *106*, 3210.
(24) Singh, U. C.; Kollman, P. A. *J. Comput. Chem.* **1986**, *7*, 718.
(25) Field, M. J.; Bash, P. A.; Karplus, M. *J. Comput. Chem.* **1990**, *11*, 700.
(26) Gao, J. L.; Xia, X. F. *Science* **1992**, *258*, 631.
(27) Gao, J. L.; Truhlar, D. G. *Annu. Rev. Phys. Chem.* **2002**, *53*, 467.
(28) Field, M. J.; Albe, M.; Bret, C.; Proust-De Martin, F.; Thomas, A. *J. Comput. Chem.* **2000**, *21*, 1088.
(29) Dewar, M. J. S.; Zoebisch, E. G.; Healy, E. F.; Stewart, J. J. P. *J. Am. Chem. Soc.* **1985**, *107*, 3902.
(30) Damm, W.; Frontera, A.; TiradoRives, J.; Jorgensen, W. L. *J. Comput. Chem.* **1997**, *18*, 1955.
(31) Jorgensen, W. L.; Chandrasekhar, J.; Madura, J. D.; Impey, R. W.; Klein, M. L. *J. Chem. Phys.* **1983**, *79*, 926.
(32) Takata, Y.; Huang, Y. F.; Komoto, J.; Yamada, T.; Konishi, K.; Ogawa, H.; Gomi, T.; Fujioka, M.; Takusagawa, F. *Biochemistry* **2003**, *42*, 8394.
(33) Kim, H. J.; Hynes, J. T. *J. Am. Chem. Soc.* **1992**, *114*, 10508.
(34) Andersen, H. C. *J. Comput. Phys.* **1983**, *52*, 24.
(35) Verlet, L. *Phys. Rev.* **1967**, *159*, 98.
(36) Roca, M.; Andres, J.; Moliner, V.; Tuñón, I.; Bertran, J. *J. Am. Chem. Soc.* **2005**, *127*, 10648.
(37) Soriano, A.; Silla, E.; Tuñón, I.; Ruiz-Lopez, M. F. *J. Am. Chem. Soc.* **2005**, *127*, 1946.
(38) Strnad, M.; MartinsCosta, M. T. C.; Millot, C.; Tuñón, I.; Ruiz-Lopez, M. F.; Rivail, J. L. *J. Chem. Phys.* **1997**, *106*, 3643.
(39) Bergsma, J. P.; Gertner, B. J.; Wilson, K. R.; Hynes, J. T. *J. Chem. Phys.* **1987**, *86*, 1356.
(40) Allen, M. P.; Tildesley, D. J. *Computer Simulations of Liquids*; Oxford: Clarendon, U.K., 1989.
(41) van der Zwan, G.; Hynes, J. T. *J. Chem. Phys.* **1982**, *76*, 2993.
(42) van der Zwan, G.; Hynes, J. T. *J. Chem. Phys.* **1983**, *78*, 4174.
(43) van der Zwan, G.; Hynes, J. T. *J. Chem. Phys.* **1984**, *90*, 21.
(44) Kramers, H. A. *Physica* **1940**, *7*, 284.
(45) Pu, J. Z.; Gao, J. L.; Truhlar, D. G. *Chem. Rev.* **2006**, *106*, 3140.
(46) Schultz, E.; Nissinen, E. *Biochem. Pharmacol.* **1989**, *38*, 3953.
(47) Warshel, A.; Hwang, J. K. *J. Chem. Phys.* **1986**, *84*, 4938.
(48) Hwang, J. K.; Chu, Z. T.; Yadav, A.; Warshel, A. *J. Phys. Chem.* **1991**, *95*, 8445.